

Enzymatically and Reductively Degradable α -Amino Acid-Based Poly(ester amide)s: Synthesis, Cell Compatibility, and Intracellular Anticancer Drug Delivery

Huanli Sun,[†] Ru Cheng,[†] Chao Deng,[†] Fenghua Meng,^{*,†} Aylvin A. Dias,[‡] Marc Hendriks,[‡] Jan Feijen,^{‡,§} and Zhiyuan Zhong^{*,†}

[†]Biomedical Polymers Laboratory, and Jiangsu Key Laboratory of Advanced Functional Polymer Design and Application, College of Chemistry, Chemical Engineering and Materials Science, Soochow University, Suzhou, 215123, People's Republic of China

[‡]DSM Biomedical, Koestraat 1, Geleen 6167 RA, The Netherlands

[§]Department of Polymer Chemistry and Biomaterials, Institute for Biomedical Technology and Technical Medicine (MIRA), Faculty of Science and Technology, University of Twente, Enschede, The Netherlands

S Supporting Information

ABSTRACT: A novel and versatile family of enzymatically and reductively degradable α -amino acid-based poly(ester amide)s (SS-PEAs) were developed from solution polycondensation of disulfide-containing di-*p*-toluenesulfonic acid salts of bis-*L*-phenylalanine diesters (SS-Phe-2TsOH) with di-*p*-nitrophenyl adipate (NA) in *N,N*-dimethylformamide (DMF). SS-PEAs with M_n ranging from 16.6 to 23.6 kg/mol were obtained, depending on NA/SS-Phe-2TsOH molar ratios. The chemical structures of SS-PEAs were confirmed by ¹H NMR and FTIR spectra. Thermal analyses showed that the obtained SS-PEAs were amorphous with a glass transition temperature (T_g) in the range of 35.2–39.5 °C. The *in vitro* degradation studies of SS-PEA films revealed that SS-PEAs underwent surface erosion in the presence of 0.1 mg/mL α -chymotrypsin and bulk degradation under a reductive environment containing 10 mM dithiothreitol (DTT). The preliminary cell culture studies displayed that SS-PEA films could well support adhesion and proliferation of L929 fibroblast cells, indicating that SS-PEAs have excellent cell compatibility. The nanoparticles prepared from SS-PEA with PVA as a surfactant had an average size of 167 nm in phosphate buffer (PB, 10 mM, pH 7.4). SS-PEA nanoparticles while stable under physiological environment undergo rapid disintegration under an enzymatic or reductive condition. The *in vitro* drug release studies showed that DOX release was accelerated in the presence of 0.1 mg/mL α -chymotrypsin or 10 mM DTT. Confocal microscopy observation displayed that SS-PEA nanoparticles effectively transported DOX into both drug-sensitive and -resistant MCF-7 cells. MTT assays revealed that DOX-loaded SS-PEA nanoparticles had a high antitumor activity approaching that of free DOX in drug-sensitive MCF-7 cells, while more than 10 times higher than free DOX in drug-resistant MCF-7/ADR cells. These enzymatically and reductively degradable α -amino acid-based poly(ester amide)s have provided an appealing platform for biomedical technology in particular controlled drug delivery applications.



INTRODUCTION

Synthetic biodegradable polymers have received continuous attention due to their wide range of applications, particularly in biomedical fields such as controlled drug release, gene transfer, and tissue engineering.^{1–5} Biodegradable aliphatic polyesters and polycarbonates due to their favorable biocompatibility and approved use in biomedical devices by the U.S. Food and Drug Administration (FDA) have become the most important synthetic biomaterials.^{6–10} However, in practice, these classical biomedical polymers often can not meet the requirements of a particular application due to their high hydrophobicity, lack of reactive centers, and improper degradation rates.

In the past decades, α -amino acid-based poly(ester amide)s (PEAs), which possess the favorable properties of both

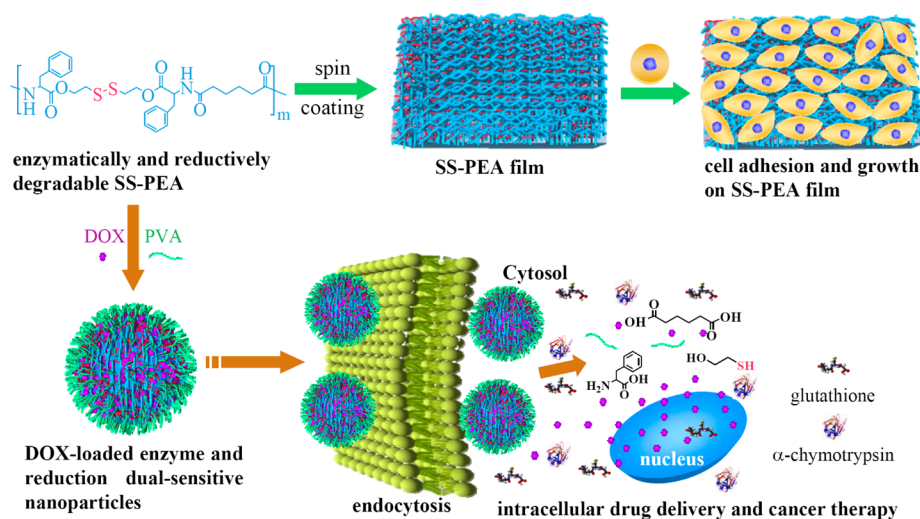
polyesters and polypeptides, such as enzymatic degradability and bioactivity, have been developed as a versatile class of biodegradable polymers.^{11–15} A series of α -amino acid-based PEAs, which contain functional groups at the side chain (such as amine, carboxyl, hydroxyl, dithiopyridyl, carbon–carbon double bond, etc.)^{16–22} or in the main chain (such as carbon–carbon double bond, oligo(ethylene glycol), poly(ϵ -caprolactone), etc.),^{23–26} have been synthesized via solution polycondensation or interfacial polymerization and studied for various biomedical applications. For example, Chu et al.

Received: November 13, 2014

Revised: December 31, 2014

Published: January 2, 2015

Scheme 1. Illustration of Enzymatically and Reductively Degradable SS-PEA Polymer for Cell Culture and Active Intracellular Anticancer Drug Delivery



synthesized PEAs bearing pendant or embedding carbon–carbon double bonds, which could provide additional functional PEA derivatives via conjugation of thiol containing molecules or bioactive agents.^{19,23} Chen et al. reported that electroactive tetraaniline grafted PEA exhibited good electroactivity, mechanical properties as well as favorable cell adhesion and growth behavior of mouse preosteoblastic MC3T3-E1 cells.²⁷ It should be noted that, despite their advantageous features and facile synthesis, there are little studies of α -amino acid-based PEAs for drug delivery applications.^{28,29}

In recent years, tremendous efforts have been directed to the development of reduction-sensitive biodegradable polymers containing disulfide bonds for efficient intracellular drug and gene delivery.^{30–35} The disulfide bonds, while stable during the circulation and in the extracellular environment, would be cleaved rapidly in the cytosol due to the presence of 2–3 orders higher level of glutathione tripeptide (GSH; about 2–10 mM) than in the extracellular fluids (about 2–20 μ M).³⁶ The fast intracellular drug release triggered by cytoplasmic GSH has shown to markedly enhance the therapeutic effects of anticancer drugs in vitro and in vivo.

In this paper, we report on the synthesis of novel enzymatically and reductively degradable L-phenylalanine based PEAs (SS-PEAs) and their applications for cell culture and anticancer drug delivery (Scheme 1). Notably, SS-PEAs exhibited excellent cell compatibility and efficient intracellular drug release resulting in effective reversal of drug resistance (ADR) in cancer cells. Herein, synthesis of SS-PEAs, cell compatibility, in vitro and intracellular release behaviors of doxorubicin (DOX)-loaded SS-PEA nanoparticles, and their antitumor activity in drug-sensitive and -resistant MCF-7 cells were investigated.

EXPERIMENTAL SECTION

Materials. SS-Phe-2TsOH was synthesized via reaction of L-phenylalanine with bis(2-hydroxyethyl)disulfide (HES) in the presence of TsOH·H₂O, and the detailed procedure is described in the Supporting Information. NA was synthesized according to Chu's work and used as dicarboxylic acid segment to afford SS-PEA. The monomer was obtained as light yellow acicular crystal with T_m at 124.1–124.5 °C, which was in accordance with the previous report.²³ L-Phenylalanine (L-Phe, 95%, J&K), bis(2-hydroxyethyl)disulfide

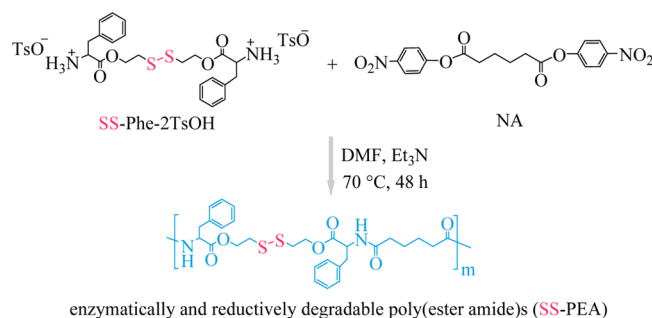
(HES, 98%, ABCR), *p*-toluenesulfonic acid monohydrate (TsOH·H₂O, 97.5%, J&K), adipoyl chloride (>98%, TCI), *p*-nitrophenol (99%, Alfa Aesar), triethylamine (Et₃N, 99%, Alfa Aesar), dithiothreitol (DTT, 99%, Merck), α -chymotrypsin from bovine pancreas (25 kDa, Sigma), poly(vinyl alcohol) (PVA, 98–99% hydrolyzed, average molecular weight 11000–31000), and doxorubicin hydrochloride (DOX·HCl, 99%, Beijing Zhongshuo Pharmaceutical Technology Development Co., Ltd.) were used as received. *N,N*-Dimethylformamide (DMF) was dried over MgSO₄ and distilled prior to use. Toluene, anhydrous methanol, acetone, ethyl acetate, chloroform, and dimethyl sulfoxide (DMSO) were used as received.

Characterization. ¹H NMR spectra were recorded on a Unity Inova 400 spectrometer operating at 400 MHz using deuterated dimethyl sulfoxide (DMSO-*d*₆) as a solvent. The chemical shifts were calibrated against residual solvent signal of DMSO-*d*₆. The molecular weight and polydispersity of the polymers were determined by a Waters 1515 gel permeation chromatograph (GPC) instrument equipped with MZ-Gel SDplus columns (500 Å) following a guard column and a differential refractive-index detector. The measurements were performed using DMF + 0.05 mol/L LiBr as the eluent at a flow rate of 0.8 mL/min at 30 °C and a series of narrow polystyrene standards for the calibration of the columns. Thermal properties of synthesized monomers and polymers were characterized using differential scanning calorimeter (DSC, Diamond DSC, Perkin Elmer). The measurements were carried out from 80 to 280 °C for monomers (T_m) and from –40 to 120 °C for SS-PEA (T_g) at a scanning rate of 10 °C/min with nitrogen flow rate of 25 mL/min. TA Universal Analysis software was used for thermal data analysis, such as the determination of melting temperature and glass transition temperature. Fourier transform infrared spectrometer (Varian 3600 FTIR) was performed on Thermo Scientific spectrophotometer with Omnic software for data acquisition and analysis. Monomers and polymers were grounded into KBr powder and pressed into discs prior to FTIR analysis. Morphology of SS-PEA films was characterized using scanning electron microscopy (S-4700, Hitachi). The size of nanoparticles was determined using dynamic light scattering (DLS). Measurements were carried out at 25 °C using Zetasizer Nano-ZS from Malvern Instruments equipped with a 633 nm He–Ne laser using backscattering detection. TEM was performed using a Tecnai G220 TEM operated at an accelerating voltage of 200 kV. The samples were prepared by dropping 10 μ L of a 0.2 mg/mL suspension of the nanoparticles on the copper grid followed by staining with phosphotungstic acid (1 wt %).

Synthesis of Enzymatically and Reductively Degradable L-Phenylalanine-Based Poly(ester amide)s (SS-PEAs). SS-PEAs bearing repeated disulfide bonds were synthesized via solution

polycondensation of SS-Phe-2TsOH and NA using Et₃N as the acid receptor for TsOH (Scheme 2). Take the synthesis of SS-PEA at a

Scheme 2. Synthesis of Reduction-Sensitive L-Phenylalanine-Based Poly(ester amide)s (SS-PEA)



NA/SS-Phe-2TsOH molar ratio of 1:1 as an example. To a Schlenk bottle equipped with a magnetic stir bar were charged SS-Phe-2TsOH (0.710 g, 0.895 mmol), NA (0.347 g, 0.895 mmol), Et₃N (0.275 mL, 1.969 mmol), and 0.471 mL of DMF. After 20 min of degassing with a nitrogen flow, the reaction vessel was sealed and immersed in an oil bath thermostated at 70 °C. The polymerization was allowed to proceed for 48 h. The resulting polymer was isolated by dilution with DMF, precipitation in ethyl acetate two times to remove *p*-nitrophenol, precipitation in water once to remove Et₃N·TsOH, and freeze-drying for 2 d. Yield: 82.5%, *M_n* (GPC) = 23.6 kg/mol, *M_w*/*M_n* = 2.4.

Reductive Degradation of SS-PEAs. Under a nitrogen atmosphere, SS-PEA (100 mg), DTT (61 mg, 0.4 mmol), and 2 mL of DMF were charged into a Schlenk bottle equipped with a magnetic stir bar. After stirring at 30 °C for predetermined intervals, aliquots of polymer solutions (e.g., 0.4 mL) were taken to obtain the degraded products via precipitation in ultrapure water, filtration, washing several times with water under a N₂ flow, and freeze-drying for 2 d. The resulting degradation products were characterized by ¹H NMR, GPC, and FTIR.

In Vitro Enzymatic and Reductive Degradation of SS-PEA Films. SS-PEA (NA/SS-Phe-2TsOH = 1:1) films were drop-cast from a 40 mg/mL chloroform solution onto glass microscope slides (1 cm × 1 cm), which was allowed to thoroughly dry by evaporation overnight at room temperature (r.t.) followed by drying in vacuo for 2 d. The films (each in duplicate) were immersed in 1 mL of PBS buffer (pH 7.4, containing 0.05 w/v% sodium azide to inhibit bacterial growth) with α-chymotrypsin (0.1 mg/mL) or 10 mM DTT in a 24-well cell culture plate and incubated at 37 °C and 120 rpm. SS-PEA films incubated in pure PBS buffer under otherwise the same conditions were used as a control. The degradation medium was refreshed every 24 h. At predetermined intervals, the remaining polymer samples (on slides) were collected via aspiration of the incubation medium followed by rinsing of the wells three times for 5 min with ultrapure water. The collected samples were then dried in vacuo to a constant weight. The degree of the degradation was estimated from the weight loss of the SS-PEA films based on the following formula:

$$\text{weight loss(\%)} = (W_0 - W_t)/W_0 \times 100\%$$

in which *W*₀ and *W_t* represent initial weight of film and weight of film at time *t*. In addition, the molecular weight and PDI of the SS-PEA films after degradation were determined by GPC.

SEM was employed to analyze the surface morphology of the SS-PEA films during the degradation process. The film preparation was the same as for weight loss experiments, except that the glass slides were changed into 0.5 cm × 0.5 cm. The SS-PEA film sample was dried and coated with gold for SEM observation.

Cell Culture on SS-PEA Films. SS-PEA films were prepared by spin-coating of SS-PEA solutions in chloroform (40 mg/mL) onto glass microscope slides (1 cm × 1 cm) and were dried in vacuo for 2 d. The films were placed into a 24-well tissue culture plate and sterilized

by immerse in 70% ethanol for 4 h accompanied by UV irradiation. The films were thoroughly rinsed with sterilized PBS to remove ethanol prior to use. L929 fibroblast cells were cultured directly on the SS-PEA films using Dulbecco's Modified Eagle Medium (DMEM) medium supplemented with 10% fetal bovine serum, 1% L-glutamine, and antibiotics penicillin (100 IU/mL) and streptomycin (100 μg/mL) at a density of 1 × 10⁴ cells/well in a humidified 5% CO₂ atmosphere at 37 °C. The culture media was 0.5 mL per well and replaced each day. After 1, 2, or 4 d of culture, the cells were observed on an inverted fluorescence microscope (Nikon ECLIPSE Ti-S).

Cell Proliferation on SS-PEA Films Using MTT Assays. L929 cells were plated into the tissue culture plate or SS-PEA films in a 24-well plate (3 × 10⁴ cells/well) using DMEM medium and incubated for different times (1–4 d). SS-PEA films with DMEM medium only were used as a control to eliminate the effect of polymer on MTT assays. At predetermined time points, 80 μL of 3-(4,5-dimethylthiazol-2-yl)-2,5-diphenyl tetrazolium bromide (MTT) solution in PBS (5 mg/mL) was added. The cells were cultured for another 4 h. The medium was aspirated, the MTT-formazan generated by live cells was dissolved in 400 μL of DMSO, and the absorbance at a wavelength of 570 nm of each well was measured using a microplate reader. Data are presented as average ± standard deviation (*n* = 3).

Preparation of SS-PEA Nanoparticles. SS-PEA nanoparticles were prepared under stirring by dropwise addition of 0.4 mL water containing 2 w/v% PVA to 0.2 mL of SS-PEA (NA/SS-Phe-2TsOH = 0.96:1) solution (2 mg/mL) in DMSO at r.t., followed by extensive dialysis (MWCO 350 kDa) against PB (10 mM, pH 7.4) for 24 h with at least 5 times change of media. The final nanoparticle concentration was about 0.5 mg/mL. The size and size distribution of the nanoparticles were determined via DLS.

Size Change of SS-PEA Nanoparticles in Response to Enzyme or DTT. The size change of nanoparticles in response to reductive or enzymatic conditions was followed by DLS measurements. Briefly, to a SS-PEA nanoparticle dispersion (0.5 mg/mL) was added a predetermined amount of α-chymotrypsin or DTT to yield a final enzyme concentration of 0.1 mg/mL or a final DTT concentration of 10 mM. The solution was placed in a shaking bed at 37 °C with a rotation speed of 200 rpm. At different time intervals, the size of the nanoparticles was determined using DLS.

Encapsulation of DOX into Nanoparticles. DOX was loaded into SS-PEA nanoparticles by dropwise addition of 0.4 mL of water containing 2 w/v% PVA to a mixture of 0.2 mL of SS-PEA solution (2 mg/mL) and DOX solution (5 mg/mL) in DMSO at varying drug/polymer weight ratios (5–30 wt %) under stirring at r.t., followed by dialysis against PB (10 mM, pH 7.4) for 8 h (MWCO 350 kDa) in the dark. The dialysis media were changed five times. For determination of drug loading content (DLC) and drug loading efficiency (DLE), lyophilized drug-loaded nanoparticles were dissolved in DMSO. The amount of DOX was determined using fluorescence (FLS920) measurement (excitation at 480 nm and emission at 560 nm). The DLC and DLE were calculated according to the following formula:

$$\text{DLC(wt\%)} = (\text{wt of loaded drug} / \text{total wt of polymer and loaded drug}) \times 100\%$$

$$\text{DLE(\%)} = (\text{weight of loaded drug} / \text{weight of drug in feed}) \times 100\%$$

Enzyme and Reduction-Triggered DOX Release. The in vitro release profiles of DOX-loaded SS-PEA nanoparticles were studied using a dialysis tube (MWCO 12000–14000) at 37 °C in three different media, that is, PB (10 mM, pH 7.4) only, PB with 0.1 mg/mL α-chymotrypsin, or PB with 10 mM DTT. In order to acquire sink conditions, drug release studies were performed at a nanoparticle concentration of 0.5 mg/mL and with 0.6 mL of nanoparticle dispersion dialysis against 20 mL of the same media. At desired time intervals, 6 mL of release media was taken out and replenished with an equal volume of fresh media. The amount of DOX released was determined by using fluorescence (FLS920) measurement (excitation

Table 1. Characteristics of Enzymatically and Reductively Degradable SS-PEA Polymers

entry	NA/SS-Phe-2TsOH (mol/mol)	$M_{n,GPC}$ (kg/mol)	$M_{w,GPC}$ (kg/mol)	PDI	T_g (°C)	yield (%)
1	1.0:1.0	23.6	56.6	2.40	39.5	82.5
2	0.98:1.0	22.3	44.1	1.97	35.2	65.7
3	0.96:1.0	21.8	36.6	1.68	37.0	63.0
4	0.93:1.0	16.6	24.0	1.45	37.5	62.9

at 480 nm). The release experiments were conducted in triplicate and the results presented are the average data with standard deviations.

Cytotoxicity Assays. The antitumor activity of DOX-loaded SS-PEA nanoparticles was evaluated in human breast adenocarcinoma MCF-7 cells and P-gp overexpressing human breast adenocarcinoma cells (DOX-resistant MCF-7 cells, MCF-7/ADR) via MTT assays. The MCF-7 and MCF-7/ADR cells were seeded in a 96-well plate at a density of 1×10^4 cells/well in 90 μ L of DMEM supplemented with 10% FBS, 1% L-glutamine, and antibiotics penicillin (100 IU/mL) and streptomycin (100 μ g/mL) for 24 h. A total of 10 μ L of DOX-loaded SS-PEA nanoparticles or free DOX in PB (10 mM, pH 7.4) was added to give varying drug dosages from 0.0001 to 100 μ g/mL. The cells were cultured for another 72 h, and 10 μ L of MTT solution in PBS (5 mg/mL) was added. The cells were incubated for 4 h. The medium was aspirated, the MTT-formazan generated by live cells was dissolved in 150 μ L of DMSO, and the absorbance at a wavelength of 570 nm of each well was measured using BioTek microplate reader. The relative cell viability (%) was determined by comparing the absorbance at 570 nm with control wells containing only cell culture medium. Data are presented as average \pm standard deviation ($n = 4$). The cytotoxicity of blank SS-PEA nanoparticles following 48 h incubation was determined in a similar way using MCF-7 and MCF-7/ADR cells with various nanoparticle concentrations of 0.1–1.0 mg/mL.

Confocal Laser Scanning Microscopy (CLSM) Studies. MCF-7 and MCF-7/ADR cells were plated on microscope slides in a 24-well plate (5×10^4 cells/well) under 5% CO₂ atmosphere at 37 °C using DMEM medium supplemented with 10% FBS, 1% L-glutamine, and antibiotics penicillin (100 IU/mL) and streptomycin (100 μ g/mL) for 24 h. A total of 50 μ L of DOX-loaded SS-PEA nanoparticles or free DOX (dosage: 20 μ g/mL) was added. After incubation for 3 h, the culture medium was removed and the cells were washed 3 times with PBS. The cells were fixed with 4% paraformaldehyde for 15 min and washed 3 times with PBS. The cell nuclei were stained with 4',6-diamidino-2-phenylindole (DAPI, blue) for 15 min and washed 4 times with PBS. The images of cells were obtained using a confocal laser scanning microscope (TCS SP2).

RESULTS AND DISCUSSION

Synthesis of Enzymatically and Reductively Degradable SS-PEAs. SS-PEAs were readily synthesized via solution polycondensation of NA and SS-Phe-2TsOH in the presence of Et₃N under mild conditions (Scheme 2). SS-Phe-2TsOH was obtained as white crystals by reacting disulfide-containing diol (HES) with L-phenylalanine in the presence of TsOH·H₂O followed by recrystallization from methanol/water (1:1 v/v). The structure of the SS-Phe-2TsOH monomer was confirmed by ¹H NMR and FTIR (Supporting Information, Figures S1 and S2A). The results of polymerization are summarized in Table 1. The polymerization was performed at four NA/SS-Phe-2TsOH molar ratios from 0.93:1 to 1.0:1. FTIR spectrum revealed that new characteristic absorption bands at ~ 1638 and 3430 cm^{-1} assignable to a C=O stretch and a NH stretch of amide groups were clearly detected in addition to C=O stretch of ester groups ($\sim 1735\text{ cm}^{-1}$; Figure S2B). ¹H NMR displayed signals assignable to NA moieties (δ 2.00 and 1.33) and SS-Phe moieties (δ 2.86, 3.01, 4.24, 4.45, 7.20, and 8.24) but no peaks ascribed to TsOH (Figure 1A). The integral ratio of signals at δ 2.00 and 4.45 pointed to an equivalent polycondensation between NA and SS-Phe-2TsOH. GPC (polystyrene as

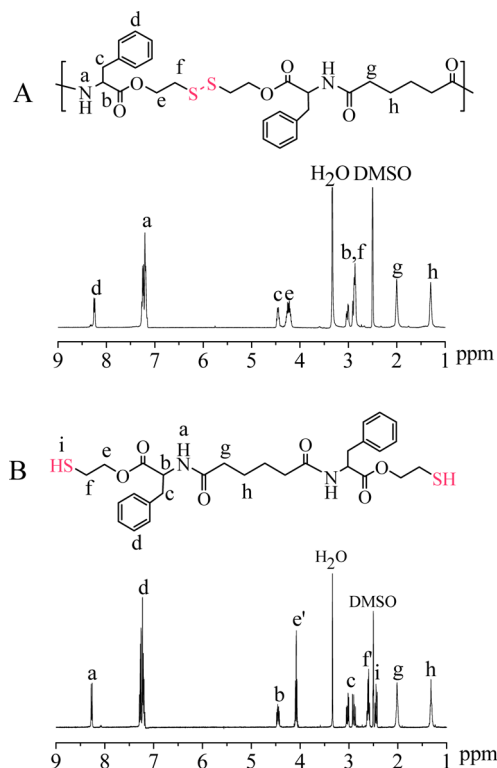


Figure 1. ¹H NMR spectra (400 MHz, DMSO-*d*₆) of (A) SS-PEA and (B) SS-PEA after treatment with DTT for 23 h.

standards) revealed that M_n of SS-PEAs varied from 16.6 to 23.6 kg/mol, which increased with increasing NA/SS-Phe-2TsOH ratios from 0.93:1 to 1.0:1 (Table 1). The molecular weight distribution was moderate ($M_w/M_n = 1.45$) at a low NA/SS-Phe-2TsOH ratio of 0.93:1. The DMSO solution of all four SS-PEAs turned into blue color following 10 min reaction with ninhydrin at 90 °C, indicating the existence of primary amine end groups. DSC measurements showed that SS-PEAs had a glass transition temperature (T_g) of 35.2–39.5 °C (Table 1), which was lower than corresponding PEAs based on 1,6-hexanediol ($T_g = 49$ °C).³⁷ The lower T_g of SS-PEAs is most likely related to their more flexible main chain resulting from the presence of multiple disulfide bonds along the backbone.

Reductive Degradation of SS-PEAs. The reductive cleavage of disulfide bonds in the repeating units of SS-PEA was investigated in DMF at 30 °C using DTT as a reducing agent. ¹H NMR and GPC measurements confirmed successful cleavage of disulfide bonds to afford small molecules after 23 h. The resonances at δ 4.24 and 2.86 attributable to the methylene protons neighboring to the ester ($-\text{COO}-\text{CH}_2-\text{CH}_2-\text{SS}-$) and disulfide bond ($-\text{CH}_2-\text{SS}-\text{CH}_2-$) shifted to δ 4.08 and 2.60, respectively, upon cleavage of disulfide bonds (Figure 1B). In addition, a new peak assignable to the thiol protons was detected at δ 2.44. The percentage of disulfide cleavage in SS-PEA polymer was determined, by comparing the integrals of peaks at δ 4.08 and 4.45, to be about 46, 55, 70.5, 86.5, and

100% following 2.5, 5, 8, 11, and 23 h treatment with DTT, respectively. GPC measurements revealed no eluent peak for SS-PEA after 23 h of treatment with DTT, supporting complete reductive degradation of polymer.

In Vitro Enzymatic and Reductive Degradation of SS-PEA Films. The enzymatic and reductive degradation kinetics of SS-PEA films were investigated in α -chymotrypsin (0.1 mg/mL) or DTT solution (10 mM) in PBS at pH 7.4. As expected, SS-PEA films exhibited slow hydrolysis in pure PBS buffer with less than 15% weight loss in 30 d (Figure 2), similar to α -amino

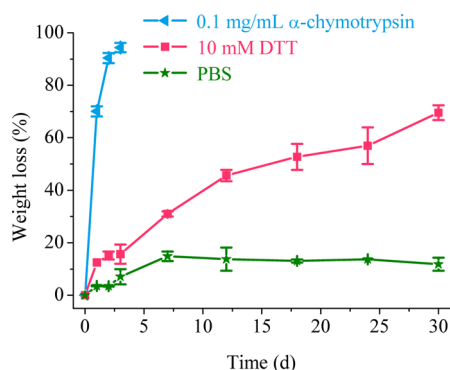


Figure 2. Percentage of SS-PEA film weight loss as a function of degradation time (d) in PBS containing 0.1 mg/mL α -chymotrypsin or 10 mM DTT at 37 °C and 120 rpm.

acid based PEAs reported previously.^{26,38,39} In contrast, fast weight loss occurred in the presence of α -chymotrypsin, in which 70 and 94% weight loss were observed in 1 and 3 d, respectively. SS-PEA films showed also much faster weight loss (16% in 3 d and 70% in 30 d) in 10 mM DTT than in PBS. It is clear, therefore, that SS-PEAs are prone to both enzymatic and reductive degradation.

To further study the degradation behaviors of SS-PEAs, molecular weights of SS-PEA film residues following enzymatic or reductive degradation were determined by GPC. The results showed that though α -chymotrypsin caused significant weight loss (70%) of SS-PEA film following 1 d incubation, little change in the molecular weight and molecular weight distribution was observed for SS-PEA film residues (Table S1), which is consistent with a surface-erosion degradation mechanism.^{40,41} In contrast, no high molecular weight polymer was observed for SS-PEA film residues following 1 d incubation in 10 mM DTT, although the weight loss was only 12.5%. These results indicated that SS-PEAs are likely subject to bulk degradation under a reductive condition. The low weight loss could be due to the fact that reductive degradation products are water insoluble. Notably, SS-PEA film following 12 d hydrolytic degradation (14% weight loss) resulted in a slight decrease in molecular weight.

The surface morphology of SS-PEA films following degradation in different media was studied using SEM (Figure S3). After 1 d incubation in pure PBS buffer, SS-PEA film showed negligible surface erosion. However, severe surface erosion was observed following treatment with α -chymotrypsin or DTT, further supporting fast enzymatic and reductive degradation. Notably, α -chymotrypsin resulted in the most significant surface erosion, in line with the weight loss data.

Formation and Triggered Disruption of SS-PEA Nanoparticles. SS-PEA nanoparticles were prepared by the solvent exchange method using PVA as a stabilizer. DLS

measurements revealed that SS-PEA polymer formed nanoparticles with average size of about 167 nm, low polydispersity of 0.08 (Figure 3 and Table S2). TEM showed that these nanoparticles had a spherical morphology (Figure 3A). Zeta potential measurements revealed a negative zeta potential of -8.9 mV.

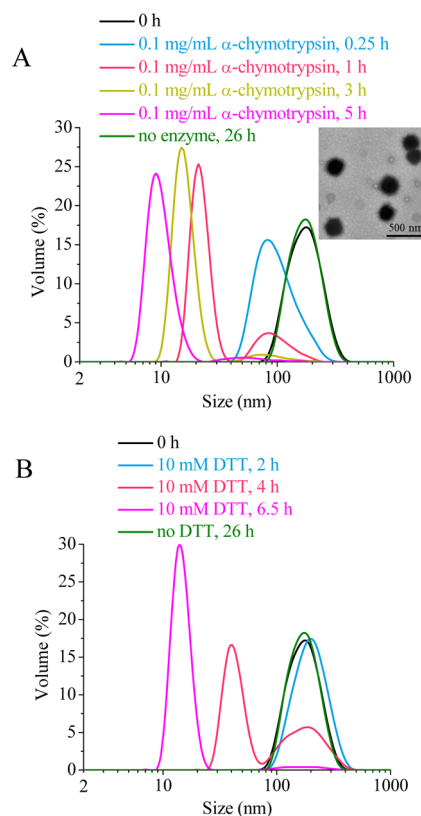


Figure 3. Change of SS-PEA nanoparticle size in response to (A) 0.1 mg/mL α -chymotrypsin and (B) 10 mM DTT determined by DLS. The inset in A represents the TEM image of SS-PEA nanoparticles.

The change of SS-PEA nanoparticle sizes in response to 0.1 mg/mL α -chymotrypsin or 10 mM DTT was studied in PB buffer (10 mM, pH 7.4) using DLS. Notably, α -chymotrypsin caused fast disintegration of SS-PEA nanoparticles, in which nanoparticle size decreased quickly with time yielding 8.7 nm unimers after 5 h (Figure 3A). Similarly, fast disruption of nanoparticles was also detected under a reductive condition containing 10 mM DTT, wherein nanoparticle size decreased to 14 nm in 6.5 h (Figure 3B). In contrast, little change in nanoparticle sizes was discerned in 26 h in the absence of DTT and α -chymotrypsin under otherwise the same conditions.

Cell Compatibility Studies. The cell compatibility of SS-PEAs was studied by culturing L929 fibroblast cells on SS-PEA films for 4 d as well as incubating MCF-7 and MCF-7/ADR cells with SS-PEA nanoparticles for 2 d. The results showed that SS-PEA film, similar to the tissue culture plate control, well supported the adhesion and growth of L929 cells (Figure 4), indicating that SS-PEA film was nontoxic, as reported for other α -amino acid-based poly(ester amide)s.^{42–45} The proliferation of L929 fibroblast cells on SS-PEA film was quantitatively determined by MTT assays. Notably, cells cultured on SS-PEA film exhibited similar proliferation rate to that for tissue culture plate from 1 to 4 d (Figure 5), further confirming that SS-PEAs are compatible to cells. Interestingly, MTT assays of SS-PEA

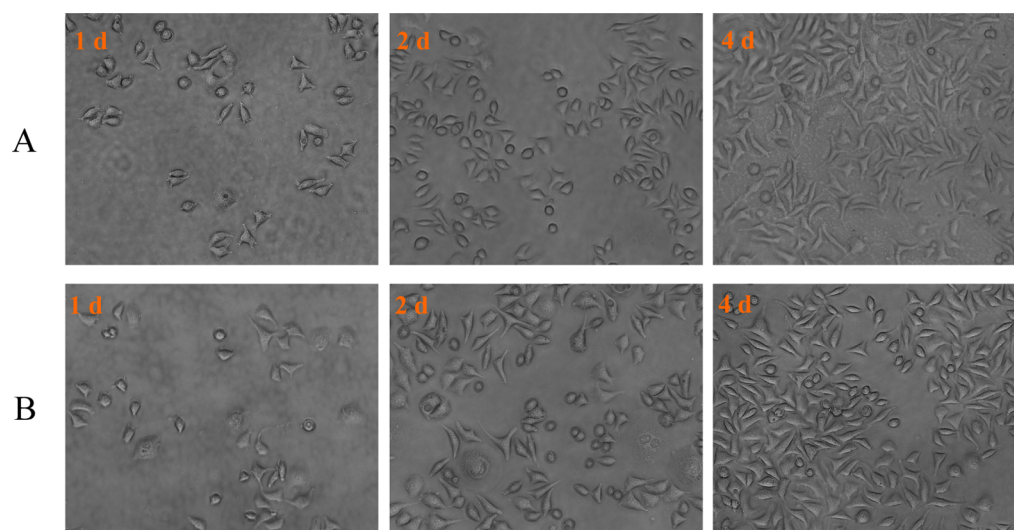


Figure 4. Phase contrast images ($\times 20$) of L929 fibroblast cells seeded at 1×10^4 cells/well after 1, 2, and 4 d culture on SS-PEA film (A) and tissue culture plate control (B). SS-PEA films had a dimension of $1 \times 1 \text{ cm}^2$.

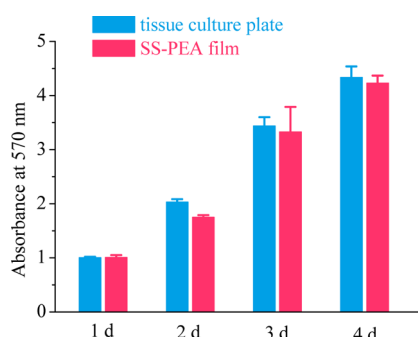


Figure 5. L929 fibroblast cell adhesion and proliferation. The cells were cultured at 1×10^4 cells/well on tissue culture plate (control) and SS-PEA films for 1, 2, 3, and 4 d. Data are presented as average \pm standard deviation ($n = 3$).

nanoparticles in MCF-7 and MCF-7/ADR cells also revealed high cell viabilities (ranging from 92.4 to 115.2%) up to a tested nanoparticle concentration of 1.0 mg/mL following 2 d incubation (Figure 6), supporting that SS-PEAs have excellent cell compatibility.

Loading and Triggered Release of DOX. DOX was loaded into SS-PEA nanoparticles at theoretical drug loading

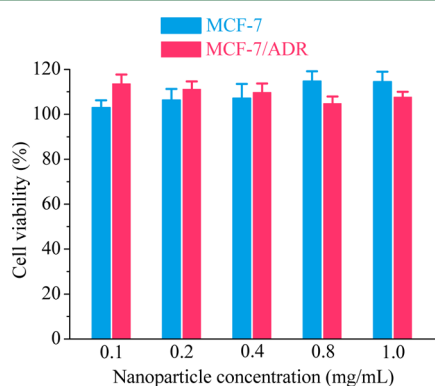


Figure 6. Cytotoxicity of SS-PEA nanoparticles toward MCF-7 and MCF-7/ADR cells. The cells are incubated with nanoparticles for 48 h. Data are presented as the average \pm standard deviation ($n = 4$).

contents (DLC) of 5, 10, 20, and 30 wt %. The results showed that SS-PEA nanoparticles could achieve a high DOX loading content of 17.3 wt % (Table S2). DLS showed that DOX-loaded SS-PEA nanoparticles had a low PDI of 0.04–0.07 and average sizes ranging from 169 to 182 nm, depending on drug contents. Remarkably, in vitro release studies revealed accelerated DOX release from SS-PEA nanoparticles in the presence of 0.1 mg/mL α -chymotrypsin or 10 mM DTT, in which about 84 and 79% of DOX was released in 24 h, respectively (Figure 7). In comparison, only about 45% of

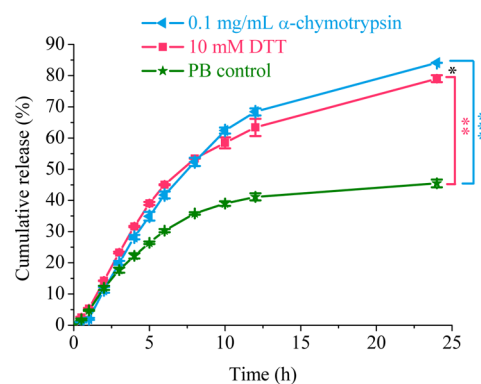


Figure 7. Enzyme or reduction triggered release of DOX from SS-PEA nanoparticles. PB (phosphate buffer, 10 mM, pH 7.4) only was used as a control. Data are presented as the average \pm standard deviation ($n = 3$; Student's t test, * $p < 0.05$, ** $p < 0.01$, *** $p < 0.001$).

DOX was released in 24 h in PB buffer under otherwise the same conditions. These results point out that drug release from SS-PEA nanoparticles is promoted by enzyme or a reductive condition.

Intracellular DOX Delivery and Antitumor Activity of DOX-Loaded SS-PEA Nanoparticles. The cellular uptake and intracellular drug release behaviors of DOX-loaded SS-PEA nanoparticles were investigated using CLSM in both MCF-7 and MCF-7/ADR cells. Interestingly, strong DOX fluorescence was observed in MCF-7 cells following a 3 h incubation with DOX-loaded SS-PEA nanoparticles (Figure 8A), indicating fast internalization of nanoparticles and rapid release of DOX inside

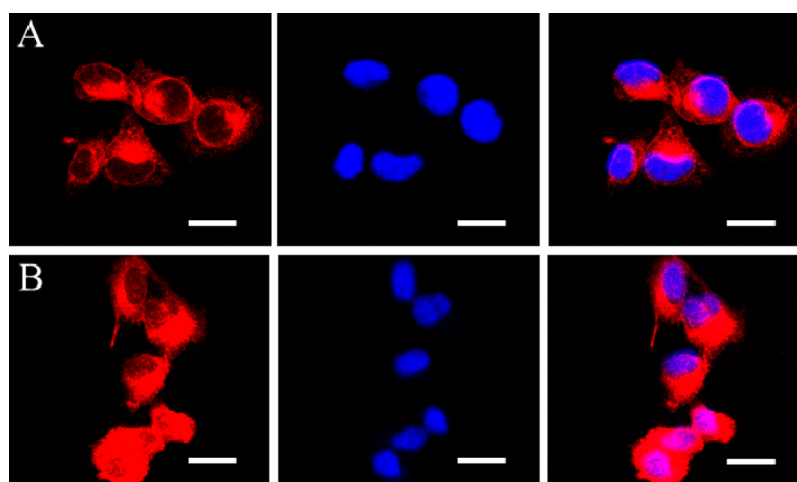


Figure 8. CLSM images of (A) MCF-7 and (B) MCF-7/ADR cells incubated with DOX-loaded SS-PEA nanoparticles (DOX dosage: 20 $\mu\text{g}/\text{mL}$) for 3 h at 37 $^{\circ}\text{C}$. For each panel, images from left to right show DOX fluorescence in cells (red), cell nuclei stained by DAPI (blue), and overlays of three images. The scale bars correspond to 20 μm in all the images.

cells. Remarkably, CLSM observations showed that DOX-loaded SS-PEA nanoparticles could also effectively transport and release DOX into the cytosol and nuclei of MCF-7/ADR cells in 3 h (Figure 8B). In comparison, negligible DOX fluorescence was observed in MCF-7/ADR cells treated with free DOX under otherwise the same conditions (Figure S4B). It is evident that enzyme and reduction dual-responsive SS-PEA nanoparticles can markedly enhance the drug concentration in MDR cancer cells, which might effectively overcome drug resistance.

The antitumor activity of DOX-loaded SS-PEA nanoparticles was investigated via MTT assays in MCF-7 and MCF-7/ADR cells. The results revealed that DOX-loaded SS-PEA nanoparticles exhibited a high antitumor effect to MCF-7 cells with a low half-maximal inhibitory concentration (IC_{50}) of 1.47 μg DOX equiv/mL following 72 h incubation, which was approaching to that for free DOX (Figure 9A). It is even more interesting to note that DOX-loaded SS-PEA nanoparticles caused also potent antitumor effect to MCF-7/ADR cells with an IC_{50} of 10.1 μg DOX equiv/mL following 72 h incubation (Figure 9B). In contrast, free DOX exhibited marginal cytotoxicity toward MCF-7/ADR cells under otherwise the same conditions (ca. 70% cell viability at a DOX dosage of 100 $\mu\text{g}/\text{mL}$), supporting strong DOX resistance. The effective reversal of drug resistance observed for DOX-loaded SS-PEA nanoparticles is likely due to their uptake by cells via endocytosis in combination with fast and efficient intracellular drug release.^{46,47} Notably, several studies showed that DOX-loaded nanoparticles exhibited several times higher antitumor activity toward MCF/ADR cells than free DOX.^{48–50} The antitumor efficacy of DOX-loaded SS-PEA nanoparticles in MCF/ADR cells was much enhanced (>10 times) as compared to free DOX, which makes it an intriguing system to overcome drug-resistance. The occurrence of drug-resistance is a major challenge for cancer chemotherapy.^{51,52} It is worthy to note that functionalization of SS-PEA nanoparticles with a specific ligand such as antibody, peptide, and aptamer might further enhance their antitumor potency.⁵³ We are convinced that SS-PEAs with facile synthesis, excellent cell compatibility, reductive and enzymatic degradability, and efficient intracellular drug release have a tremendous potential in development of multifunctional drug delivery systems.

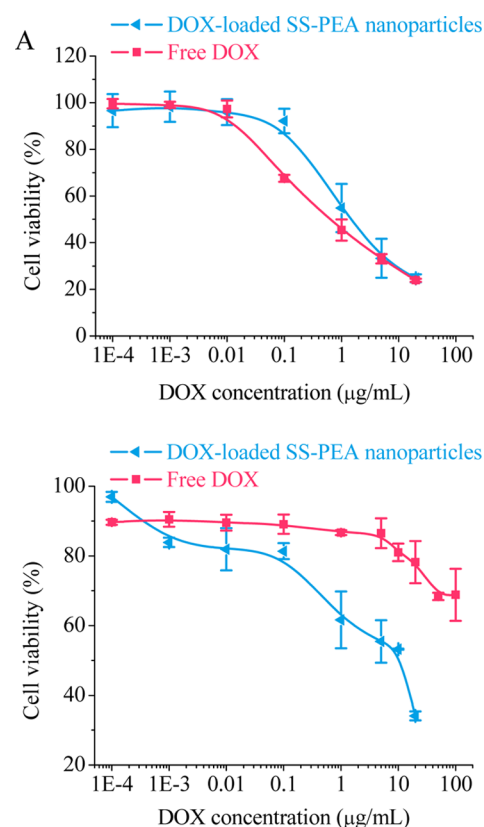


Figure 9. Antitumor activity of DOX-loaded SS-PEA nanoparticles toward MCF-7 cells (A) and MCF-7/ADR cells (B). The cells were incubated for 72 h with DOX-loaded SS-PEA nanoparticles or free DOX at varying DOX doses. Data are presented as the average \pm standard deviation ($n = 4$).

CONCLUSIONS

We have demonstrated that enzymatically and reductively degradable α -amino acid-based poly(ester amide)s (SS-PEAs) can be readily prepared under mild conditions. Notably, SS-PEAs either in the form of films or nanoparticles exhibit excellent cell compatibility, fast surface degradation by α -chymotrypsin, and bulk degradation under an intracellular-mimicking reductive environment. The initial drug loading and

release studies show that SS-PEA nanoparticles have decent loading of DOX and drug release is accelerated by α -chymotrypsin or dithiothreitol. Moreover, DOX-loaded SS-PEA nanoparticles exhibit potent antitumor efficacy toward both drug-sensitive and drug-resistant MCF-7 cells. SS-PEAs with unique properties of facile synthesis, excellent biocompatibility, enzymatic degradability, and reduction-sensitivity are of particular interest in the development of smart nanosystems for targeted cancer chemotherapy.

■ ASSOCIATED CONTENT

■ Supporting Information

Synthesis of SS-Phe-2TsOH and NA monomers; ^1H NMR spectrum of SS-Phe-2TsOH; FTIR spectra; SEM images, weight loss, and GPC data of SS-PEA films prior to and after incubation in different media; CLSM images of MCF-7 and MCF-7/ADR cells incubated with free DOX; and DOX loading results of SS-PEA nanoparticles. This material is available free of charge via the Internet at <http://pubs.acs.org>.

■ AUTHOR INFORMATION

Corresponding Authors

*Tel./Fax: +86-512-65880098. E-mail: fhmeng@suda.edu.cn.

*E-mail: zyzhong@suda.edu.cn.

Notes

The authors declare no competing financial interest.

■ ACKNOWLEDGMENTS

This work is financially supported by research grants from the National Natural Science Foundation of China (NSFC 51103093, 51173126, and 51473111), the National Science Fund for Distinguished Young Scholars (NSFC 51225302), and a Project Funded by the Priority Academic Program Development (PAPD) of Jiangsu Higher Education Institutions.

■ REFERENCES

- Huebsch, N.; Mooney, D. J. *Nature* **2009**, *462*, 426–432.
- Nair, L. S.; Laurencin, C. T. *Prog. Polym. Sci.* **2007**, *32*, 762–798.
- Tian, H.; Tang, Z.; Zhuang, X.; Chen, X.; Jing, X. *Prog. Polym. Sci.* **2012**, *37*, 237–280.
- Serrano, M. C.; Chung, E. J.; Ameer, G. A. *Adv. Funct. Mater.* **2010**, *20*, 192–208.
- Nicolas, J.; Mura, S.; Brambilla, D.; Mackiewicz, N.; Couvreur, P. *Chem. Soc. Rev.* **2013**, *42*, 1147–1235.
- Seyednejad, H.; Ghassemi, A. H.; van Nostrum, C. F.; Vermonden, T.; Hennink, W. E. *J. Controlled Release* **2011**, *152*, 168–176.
- Cameron, D. J. A.; Shaver, M. P. *Chem. Soc. Rev.* **2011**, *40*, 1761–1776.
- Gaucher, G.; Marchessault, R. H.; Leroux, J.-C. *J. Controlled Release* **2010**, *143*, 2–12.
- Feng, J.; Zhuo, R.-X.; Zhang, X.-Z. *Prog. Polym. Sci.* **2012**, *37*, 211–236.
- Chen, W.; Meng, F.; Cheng, R.; Deng, C.; Feijen, J.; Zhong, Z. *J. Controlled Release* **2014**, *190*, 398–414.
- Fonseca, A. C.; Gil, M. H.; Simões, P. N. *Prog. Polym. Sci.* **2014**, *39*, 1291–1311.
- Sun, H.; Meng, F.; Dias, A. A.; Hendriks, M.; Feijen, J.; Zhong, Z. *Biomacromolecules* **2011**, *12*, 1937–1955.
- Rodríguez-Galan, A.; Franco, L.; Puiggali, J. *Polymers* **2011**, *3*, 65–99.
- Kropp, M.; Morawa, K.-M.; Mihov, G.; Salz, A.; Harmening, N.; Franken, A.; Kemp, A.; Dias, A.; Thies, J.; Johnen, S.; Thumann, G. *Polymers* **2014**, *6*, 243–260.
- Soleimani, A.; Drappel, S.; Carlini, R.; Goredema, A.; Gillies, E. R. *Ind. Eng. Chem. Res.* **2014**, *53*, 1452–1460.
- De Wit, M. A.; Wang, Z. X.; Atkins, K. M.; Mequanint, K.; Gillies, E. R. *J. Polym. Sci., Polym. Chem.* **2008**, *46*, 6376–6392.
- Atkins, K. M.; Lopez, D.; Knight, D. K.; Mequanint, K.; Gillies, E. R. *J. Polym. Sci., Polym. Chem.* **2009**, *47*, 3757–3772.
- Deng, M. X.; Wu, J.; Reinhart-King, C. A.; Chu, C. C. *Biomacromolecules* **2009**, *10*, 3037–3047.
- Pang, X.; Chu, C. C. *Biomaterials* **2010**, *31*, 3745–54.
- Yamanouchi, D.; Wu, J.; Lazar, A. N.; Kent, K. C.; Chu, C. C.; Liu, B. *Biomaterials* **2008**, *29*, 3269–3277.
- Deng, M.; Wu, J.; Reinhart-King, C. A.; Chu, C.-C. *Acta Biomater.* **2011**, *7*, 1504–1515.
- Mejia, J. S.; Gillies, E. R. *Polym. Chem.* **2013**, *4*, 1969–1982.
- Guo, K.; Chu, C. C.; Chkhaidze, E.; Katsarava, R. *J. Polym. Sci., Polym. Chem.* **2005**, *43*, 1463–1477.
- Guo, K.; Chu, C. C. *Biomacromolecules* **2007**, *8*, 2851–2861.
- Guo, K.; Chu, C. C. *J. Appl. Polym. Sci.* **2012**, *125*, 812–819.
- Guo, K.; Chu, C. C. *J. Polym. Sci., Polym. Chem.* **2007**, *45*, 1595–1606.
- Cui, H.; Liu, Y.; Deng, M.; Pang, X.; Zhang, P.; Wang, X.; Chen, X.; Wei, Y. *Biomacromolecules* **2012**, *13*, 2881–2889.
- Guo, K.; Chu, C. C. *J. Biomed. Mater. Res., Part B* **2009**, *89*, 491–500.
- Soleimani, A.; Borecki, A.; Gillies, E. R. *Polym. Chem.* **2014**, *5*, 7062–7071.
- Sun, H.; Guo, B.; Cheng, R.; Meng, F.; Liu, H.; Zhong, Z. *Biomaterials* **2009**, *30*, 6358–6366.
- Kim, T.-i.; Ou, M.; Lee, M.; Kim, S. W. *Biomaterials* **2009**, *30*, 658–664.
- Meng, F.; Hennink, W. E.; Zhong, Z. *Biomaterials* **2009**, *30*, 2180–2198.
- Nelson-Mendez, A.; Aleksanian, S.; Oh, M.; Lim, H. S.; Oh, J. K. *Soft Matter* **2011**, *7*, 7441–7452.
- Phillips, D. J.; Gibson, M. I. *Biomacromolecules* **2012**, *13*, 3200–3208.
- Lu, H.; Sun, P.; Zheng, Z.; Yao, X.; Wang, X.; Chang, F.-C. *Polym. Degrad. Stab.* **2012**, *97*, 661–669.
- Schafer, F. Q.; Buettner, G. R. *Free Radic. Biol. Med.* **2001**, *30*, 1191–1212.
- Katsarava, R.; Beridze, V.; Arabuli, N.; Kharadze, D.; Chu, C. C.; Won, C. Y. *J. Polym. Sci., Polym. Chem.* **1999**, *37*, 391–407.
- Tsitlanadze, G.; Machaidze, M.; Kviria, T.; Djavakhishvili, N.; Chu, C. C.; Katsarava, R. *J. Biomater. Sci., Polym. Ed.* **2004**, *15*, 1–24.
- Guo, K.; Chu, C. C. *Biomaterials* **2007**, *28*, 3284–3294.
- Fan, Y. J.; Kobayashi, M.; Kise, H. *J. Polym. Sci., Polym. Chem.* **2001**, *39*, 1318–1328.
- Ghaffar, A.; Draaisma, G. J. J.; Mihov, G.; Dias, A. A.; Schoenmakers, P. J.; van der Wal, S. *Biomacromolecules* **2011**, *12*, 3243–3251.
- Horwitz, J. A.; Shum, K. M.; Bodle, J. C.; Deng, M.; Chu, C.-C.; Reinhart-King, C. A. *J. Biomed. Mater. Res., Part A* **2010**, *95*, 371–380.
- Wu, J.; Chu, C.-C. *J. Mater. Chem. B* **2013**, *1*, 353–360.
- Knight, D. K.; Gillies, E. R.; Mequanint, K. *Acta Biomater.* **2014**, *10*, 3484–3496.
- Said, S.; Pickering, J. G.; Mequanint, K. *Pharm. Res.* **2014**, *31*, 3335–3347.
- Wang, Y. C.; Wang, F.; Sun, T. M.; Wang, J. *Bioconjugate Chem.* **2011**, *22*, 1939–1945.
- Zhong, Y.; Wang, C.; Cheng, L.; Meng, F.; Zhong, Z.; Liu, Z. *Biomacromolecules* **2013**, *14*, 2411–2419.
- Wang, F.; Wang, Y.-C.; Dou, S.; Xiong, M.-H.; Sun, T.-M.; Wang, J. *ACS Nano* **2011**, *5*, 3679–3692.
- Wang, H.; Zhao, Y.; Wang, H.; Gong, J.; He, H.; Shin, M. C.; Yang, V. C.; Huang, Y. *J. Controlled Release* **2014**, *192*, 47–56.
- Tian, G.; Zheng, X.; Zhang, X.; Yin, W.; Yu, J.; Wang, D.; Zhang, Z.; Yang, X.; Gu, Z.; Zhao, Y. *Biomaterials* **2015**, *40*, 107–116.
- Holohan, C.; Van Schaeybroeck, S.; Longley, D. B.; Johnston, P. G. *Nat. Rev. Cancer* **2013**, *13*, 714–726.

(52) Patel, N. R.; Pattni, B. S.; Abouzeid, A. H.; Torchilin, V. P. *Adv. Drug Delivery Rev.* **2013**, *65*, 1748–1762.

(53) Zhong, Y.; Meng, F.; Deng, C.; Zhong, Z. *Biomacromolecules* **2014**, *15*, 1955–1969.